# A 3-D reduced fracture model for two-phase flow in porous media with a global pressure formulation

Elyes Ahmed, Jérôme Jaffré, Jean E. Roberts

MAMERN VI–2015: $6^{th}$ International Conference on Approximation Methods
and Numerical Modelling in Environment and Natural Resources
Pau (France), June 1-5, 2015

# A 3-D reduced fracture model for two-phase flow in porous media with a global pressure formulation

**Elyes Ahmed**[1,2]**, Jérôme Jaffré**[2] **and Jean E. Roberts**[2]

[1]ENIT-Lamsin, University of Tunis El Manar, Tunisia
ahmed_elyes@yahoo.com

[2]INRIA Paris-Rocquencourt, France

**Keywords:** porous media, two-phase flow, fractures

**Abstract.** *We consider three-dimensional incompressible two-phase flow in a porous medium with fractures. Interaction between the fractures and the rock matrix is taken into account. The location, the geometry and the rock properties of the fractures are considered known (discrete model) and the fractures are modeled as two-dimensional interfaces (reduced model). The fractures and the rock matrix have different rock types. Two-phase flow is modeled using the global pressure formulation. The model is presented and numerical experiments are shown.*

## 1 Introduction

The presence of fractures in a porous medium greatly complicates the modeling of flow and transport in porous media. Fractures occur at different scales with different geometries, and they may behave as either channels or barriers for the fluid flow. Therefore the fractures have a very strong influence on flow and transport, either making flow in certain directions several orders of magnitude more rapid than in others or possibly blocking flow in certain directions. There is a need for complex simulation models that simulate fluid flow

along fractures as well as the interchange of fluid between fractures and the surrounding porous rock matrix.

There are continuous models of fractures which deal with a large number of fractures through an averaging or homogenizing process, but we are considering here a discrete fracture model in which the locations of the fractures are given and we take into account matrix-fracture interaction. The difficulties in the numerical modeling of multiphase flow in a porous medium with fractures stem from the heterogeneity and anisotropy of the fracture-matrix system as well as its nonlinearities which change with the rock type. In order to deal with these difficulties, reduced fracture models treat fractures as $(n-1)-$dimensional objects embedded in an $n-$dimensional medium, $n$ being either 2 or 3. A number of articles have been written on numerical models of this type; see [8, 10, 9, 7, 4, 12] and references therein. Here, we are interested in locally mass conserving methods and in particular in mixed finite element methods or cell centered finite volume methods. The object of this work is to extend the two-phase flow model presented in [7] and to discuss numerical experiments.

After this introduction we present in Section 2 the formulation of incompressible two-phase flow using the global pressure. In Section 3 we present the reduced fracture model of incompressible two-phase flow in a fractured domain for which the fracture is modeled as an interface between subdomains in the surrounding rock matrix. Section 4 describes shortly numerical methods and some implementation issues. A numerical experiment is shown in Section 5.

## 2 Global pressure formulation of incompressible two-phase flow

We consider incompressible two-phase flow in a porous medium. The index for the wetting phase is $\ell = w$ and $\ell = nw$ is that for the nonwetting phase. The unknown quantities are the phase saturations $s_\ell$ and pressures $p_\ell$, as well as the Darcy velocities $\mathbf{u}_\ell$. We assume that the volume of all pores is filled by the two phases, implying

$$s_n + s_{nw} = 1, \tag{1}$$

and we choose for the main saturation unknown the saturation of the wetting phase $s = s_w$.

The saturation equation expresses volume conservation for each fluid phase (which is equivalent to mass conservation since the fluids are assumed to be incompressible):

$$\Phi \frac{\partial s_\ell}{\partial t} + \nabla \cdot \mathbf{u}_\ell = q_\ell, \qquad \ell \in \{w, nw\}, \tag{2}$$

where the $q_\ell$'s are the source terms given as functions of the wetting phase saturation ($0 \le s \le 1$ ) and $\Phi$ is the porosity. The phase Darcy velocities $\mathbf{u}_\ell$'s satisfy Darcy's law

$$\mathbf{u}_\ell = -\mathbf{K}\, k_\ell(s)(\nabla p_\ell - \rho_\ell \mathbf{u}_G), \qquad \ell \in \{w, nw\}, \tag{3}$$

where $\mathbf{K}$ denotes the tensor of absolute permeabilities, $\rho_\ell$ and $k_\ell$ are the phase densities and the phase mobilities, respectively, and $\mathbf{u}_G$ denotes the gravity field. The mobilities are positive monotone functions of the saturation $s$: $k_w$ is increasing and $k_w(0) = 0$, while $k_{nw}$ is decreasing and $k_{nw}(1) = 0$.

The difference between the phase pressures is the capillary pressure $\pi$

$$\pi(s) = p_{nw} - p_w, \tag{4}$$

and $\pi$ is a positive decreasing function of $s$.

The capillary pressure curve $\pi$ and the relative permeability curves $k_\ell$, $\ell = w, nw$, depend on the physical properties of the two phases and the rock. Standard models for capillary pressure and relative permeabilities are those of Muelam-Van Genuchten and Brooks-Corey. More details on two-phase flow in porous media can be found in [5].

To present the global pressure formulation we follow [3]. We introduce the total velocity $\mathbf{u}$ which is the sum of the Darcy velocities of the wetting and the nonwetting phases

$$\mathbf{u} = \mathbf{u}_w + \mathbf{u}_{nw} = -\sum_{\ell \in \{w, nw\}} \mathbf{K}\, k_\ell(s)(\nabla p_\ell - \rho_\ell \mathbf{u}_G). \tag{5}$$

We then add equations (2) for $\ell = w, n$, which because of (1) yields

$$\nabla \cdot \mathbf{u} = q_{nw}(1 - s) + q_w(s) = q(s). \tag{6}$$

. We introduce the following functions of saturation

$$\alpha(s) = \int_0^s a(\sigma) d\sigma, \quad a(s) = -\frac{k_w k_{nw}}{k_w + k_{nw}} \pi'(s),$$

and we note that $a(0) = a(1) = 0$ and that $\alpha(0) = 0$.

We rewrite the Darcy velocity of the wetting phase as

$$\mathbf{u}_w = -\mathbf{K}\, \nabla \alpha(s) + f_w(s)\Big(\mathbf{u} + f_{Gw}(s)\mathbf{K}\mathbf{u}_G\Big), \tag{7}$$

where the nonlinear functions $f_w$ and $f_{Gw}$ are defined by

$$\begin{aligned} &f_w(s) = \frac{k_w(s)}{k(s)}, \;\; k(s) = k_w(s) + k_{nw}(s), \\ &f_{Gw}(s) = k_{nw}(s)(\rho_w - \rho_{nw}). \end{aligned} \tag{8}$$

Thus, $\mathbf{u}_w$ is the sum of a capillary diffusion contribution $\mathbf{r} = -\mathbf{K}\,\nabla\alpha(s)$, and an advection contribution $\mathbf{f} = f_w(s)\Big(\mathbf{u} + f_{Gw}(s)\mathbf{K}\mathbf{u}_G\Big)$. Note that the Darcy velocity of the non wetting phase can now be written as

$$\mathbf{u}_{nw} = \mathbf{u} - \mathbf{u}_w = \mathbf{K}\,\nabla\alpha(s) + f_{nw}(s)\Big(\mathbf{u} + f_{Gnw}(s)\mathbf{K}\mathbf{u}_G\Big) \tag{9}$$

with

$$f_{nw}(s) = \frac{k_{nw}(s)}{k(s)},\ f_{Gnw}(s) = k_w(s)(\rho_{nw} - \rho_w). \tag{10}$$

The saturation equations can now be written as

$$\Phi\frac{\partial s}{\partial t} + \nabla\cdot\mathbf{u}_w = q_w, \quad \mathbf{u}_w = \mathbf{r} + \mathbf{f}, \tag{11}$$

$$\mathbf{r} = -\mathbf{K}\,\nabla\alpha(s), \quad \mathbf{f} = f_w(s)\Big(\mathbf{u} + f_{Gw}(s)\mathbf{K}\mathbf{u}_G\Big). \tag{12}$$

Still following [3], we introduce the global pressure $p$, as a main unknown, defined by

$$p = \frac{1}{2}(p_w + p_{nw}) + \beta(s), \tag{13}$$

where $\beta$ is the function $\beta(s) = \displaystyle\int_1^s (\frac{1}{2} - f_w(\sigma))\pi'(\sigma)\,d\sigma$. Using equations (4)-(13) we can write the phase pressures in terms of the capillary pressure and the global pressure

$$p_w = p - \beta(s) - (1/2)\pi(s), \quad p_{nw} = p - \beta(s) + (1/2)\pi(s). \tag{14}$$

Using the global pressure the total Darcy velocity $\mathbf{u}$ satifies an extended Darcy law

$$\mathbf{u} = -\mathbf{K}\,k(s)\,(\nabla p - \rho(s)\mathbf{u}_G),$$

where

$$\rho = \frac{k_w\rho_w + k_{nw}\rho_{nw}}{k}. \tag{15}$$

The global pressure is not a physical pressure and is only a mathematical tool. It is a smooth function defined in the whole domain, whether a phase vanishes or not. It satisfies $p = p_w$ if $s_w = 1$, $p = p_{nw}$ if $s_w = 0$, and $p_w \le p \le p_{nw}$ when the two phases are present. Finally, the total Darcy velocity $\mathbf{u}$ and the global pressure $p$ satify the pressure equation

$$\nabla\cdot\mathbf{u} = q(s), \tag{16}$$

$$\mathbf{u} = -\mathbf{K}\,k(s)\,(\nabla p - \rho(s)\mathbf{u}_G). \tag{17}$$

We suppose that the domain $\Omega \subset \mathbb{R}^3$ contains a fracture $\Omega_f$ which separates $\Omega$ into two subdomains $\Omega_1$ and $\Omega_2$ which are the rock matrix, $\Omega = \Omega_1 \cup \Omega_f \cup \Omega_2$.

We use the following division of the boundary, a Dirichlet part $\Gamma^{sD}$ and a Neumann part $\Gamma^{sN}$ for the saturation equation, and similarly a Dirichlet part $\Gamma^{pD}$ and a Neumann part $\Gamma^{pN}$ for the pressure equation. We also use the notation $\Gamma_i^{pN} = \Gamma^{pN} \cap \partial\Omega_i$, $\Gamma_i^{pD} = \Gamma^{pD} \cap \partial\Omega_i$, $\Gamma_i^{sN} = \Gamma^{sN} \cap \partial\Omega_i$, and $\Gamma_i^{sD} = \Gamma^{sD} \cap \partial\Omega_i$.

The fracture is supposed to be also a porous medium delimited by two surfaces $\gamma_i = \partial\Omega_f \cap \partial\Omega_i$, $i = 1, 2$. It has a width $d$ which is very small compared to the size of the whole domain $\Omega$.

The matrix rock and the fracture have different rock types, which means not only that the porosity and the absolute permeability differ but also the nonlinear capillary pressure and relative permeability functions. The subdomains are indexed by $i = 1, 2.f$ and an index $i$ for any function indicates the restriction of that function to subdomain $i$.

Across interfaces between two rock types, we assume continuity of the normal component of the Darcy velocities to preserve conservation, and continuity of the phase pressures which from equation (4) implies continuity of capillary pressure $\pi$, and from equation (13) continuity of $p - \beta$.

## 3 The reduced model for fractures

In the reduced model, the fracture $\Omega_f$ is collapsed into an interface $\gamma$ of dimension 2. The absolute permeability tensor $\mathbf{K}$ is assumed to be made up of a tangential component $\mathbf{K}_{f,\tau}$ and a normal component $K_{f,n}$. These functions characterizing the rock type of the fracture as well as the porosity $\Phi_f$ are assumed to be constant in the direction normal to $\gamma$ so they are considered as functions on $\gamma$. Also, we introduce the notation $\nabla_\tau$ and $\nabla_{\mathbf{n}}$ for the tangential and the normal components of the gradient operator. On the interface $\gamma$ we introduce the following quantities for pressure, saturation, source terms and Darcy velocities

$$
\begin{aligned}
p_\gamma &= \frac{1}{d}\int_{-d/2}^{d/2} p_f \, dn, \quad & s_\gamma &= \frac{1}{d}\int_{-d/2}^{d/2} s_f \, dn, \\
q_\gamma &= \int_{-d/2}^{d/2} q_f \, dn, & q_{w\gamma} &= \int_{-d/2}^{d/2} q_{wf} \, dn, \\
\mathbf{u}_\gamma &= \int_{-d/2}^{d/2} \mathbf{u}_{f,\tau} \, dn, & \mathbf{u}_{w\gamma} &= \int_{-d/2}^{d/2} \mathbf{u}_{wf,\tau} \, dn,
\end{aligned}
$$

where $\mathbf{u}_{f,\tau}$ and $\mathbf{u}_{wf,\tau}$ are the tangential components of $\mathbf{u}_f$ and $\mathbf{u}_{wf}$.

The reduced model consists of a set of equations in $\Omega_i$ coupled with a set of equations in $\gamma$. For more see [7, 1].

*Pressure equations in $\Omega$*

$$\nabla \cdot \mathbf{u}_i = q_i, \qquad \text{in } \Omega_i, \tag{18}$$

$$\mathbf{u}_i = -\mathbf{K}_i\, k_i(s_i)\,(\nabla p_i - \rho_i(s_i)\mathbf{u}_G), \qquad \text{in } \Omega_i, \tag{19}$$

$$-\frac{1}{\delta(s_\gamma)}\mathbf{u}_i \cdot \mathbf{n}_i + p_i - \beta_i(s_i) = p_\gamma - \beta_f(s_\gamma) \quad \text{on } \gamma, \tag{20}$$

$$\mathbf{u}_i \cdot \mathbf{n}_i = 0, \qquad \text{on } \Gamma_i^{pN}, \tag{21}$$

$$p_i = \overline{p}_D, \qquad \text{on } \Gamma_i^{pD}, \tag{22}$$

where $\delta(s_\gamma) = \frac{\mathbf{K}_{f\mathbf{n}}\, k_f(s_\gamma)}{d/2}$.

*Pressure equations in $\gamma$*

$$\nabla_\tau \cdot \mathbf{u}_\gamma = q_\gamma + \mathbf{u}_1 \cdot \mathbf{n}_1 + \mathbf{u}_2 \cdot \mathbf{n}_2, \qquad \text{in } \gamma, \tag{23}$$

$$\mathbf{u}_\gamma = -\mathbf{K}_\gamma\, k_\gamma(s_\gamma)\Big(\nabla_\tau p_\gamma - \rho_\gamma(s_\gamma)\mathbf{u}_G\Big), \qquad \text{in } \gamma, \tag{24}$$

$$p_\gamma = \overline{p}_D, \qquad \text{on } \partial\gamma. \tag{25}$$

Recalling Eq. (13), we observe that equation (20) is a Darcy law linking the total Darcy velocity to the drop of the average of the phase pressures between $\partial\Omega_i \cap \gamma$ and the middle of the fracture and in the direction normal to $\gamma$. We also note that in the conservation equation (23) for $\gamma$, with the external source term, there appears the contribution from the subdomains to the flow in the fracture.

*Saturation equations in $\Omega_i$*

$$\Phi_i \frac{\partial s_i}{\partial t} + \nabla \cdot \mathbf{u}_{wi} = q_i,\ \mathbf{u}_{wi} = \mathbf{r}_i + \mathbf{f}_i, \qquad \text{in } \Omega_i, \tag{26}$$

$$\mathbf{r}_i = -\mathbf{K}_i\, \nabla\, \alpha_i(s_i), \qquad \text{in } \Omega_i, \tag{27}$$

$$\mathbf{f}_i = f_{wi}(s_i)\Big(\mathbf{u}_i + f_{Gwi}(s_i)\mathbf{K}_i\mathbf{u}_G\Big), \qquad \text{in } \Omega_i, \tag{28}$$

$$\frac{1}{\delta_w(s_\gamma)}\mathbf{u}_{wi} \cdot \mathbf{n}_i + \frac{\pi_i(s_i)}{2} = \frac{\pi_\gamma}{2}(s_\gamma) + \frac{1}{\delta(s_\gamma)}\mathbf{u}_i \cdot \mathbf{n}_i, \text{on } \gamma, \tag{29}$$

$$\mathbf{u}_{wi} \cdot \mathbf{n}_i = 0, \qquad \text{on } \Gamma_i^{sN}, \tag{30}$$

$$s_i = \overline{s}_D, \qquad \text{on } \Gamma_i^{sD}, \tag{31}$$

where $\delta_w(s_\gamma) = \dfrac{\mathbf{K}_{f\mathbf{n}}\, k_{wf\mathbf{n}}(s_f)}{d/2}$.

*Saturation equations in $\gamma$*

$$\Phi_\gamma \frac{\partial s_\gamma}{\partial t} + \nabla_\tau \cdot \mathbf{u}_{w\gamma} = q_{w\gamma} + \mathbf{u}_{w1} \cdot \mathbf{n}_1 + \mathbf{u}_{w2} \cdot \mathbf{n}_2, \quad \text{in } \gamma, \tag{32}$$

$$\mathbf{u}_{w\gamma} = \mathbf{r}_\gamma + \mathbf{f}_\gamma, \quad \text{in } \gamma, \tag{33}$$

$$\mathbf{r}_\gamma = -\mathbf{K}_\gamma \nabla_\tau \alpha_f(s_\gamma), \quad \text{in } \gamma, \tag{34}$$

$$\mathbf{f}_\gamma = f_{w\gamma}(s_\gamma)\Big(\mathbf{u}_\gamma + f_{Gw\gamma}(s_\gamma)\mathbf{K}_\gamma \mathbf{u}_G\Big), \quad \text{in } \gamma, \tag{35}$$

$$\mathbf{u}_{w\gamma} \cdot \mathbf{n}_\gamma = 0, \quad \text{on } \Gamma_\gamma^{sN}, \tag{36}$$

$$s_\gamma = \overline{s}_D, \quad \text{on } \Gamma_\gamma^{sD}. \tag{37}$$

where $\Phi_\gamma = d\Phi_f$. We can make similar comments for the saturation equations to those made for the pressure equations. Eq. (29) is a Darcy law linking the Darcy velocity for the wetting fluid to the drop of the wetting phase pressure between $\partial\Omega_i \cap \gamma$ and the middle of the fracture and in the direction normal to $\gamma$. Indeed using Eqs. (20), (13), (4) Eq,(29) is equivalent to $\dfrac{1}{\delta_w(s_\gamma)}\mathbf{u}_{wi} \cdot \mathbf{n}_i = p_{wi} - p_{w\gamma}$.

Finally one should note that this model works for a fracture with a larger absolute permeability than that in the rock matrix as well as a fracture with a smaller absolute permeability (barrier).

## 4 Numerical methods and implementation

For time discretization we use an Euler first order discretization of the IMPES type (IMplicit Pressure Explicit Saturation). That is in the pressure equation, the saturation are left at the previous time level. Therefore the pressure equation and the saturation equation are decoupled and solved one after the other. For the saturation equation we split capillary diffusion and advection, so diffusion can be treated implicitly while advection is treated explicitly and we use different time steps for diffusion and advection. Since advection is calculated with an Euler explicit method, the advection time step must be bounded by a CFL condition to preserve the stability of the scheme. On the contrary the diffusion time step is not bounded by stability considerations but only by accuracy considerations. Since very often advection is dominant the diffusion time step is usually larger than the advection time step.

Furthermore since the matrix domain and the fracture may have very different physical properties one would like to use different time steps in the matrix domain and in the fracture, smaller time steps in the matrix domain when the fracture is a barrier (having smaller permeability) and smaller time steps in the

fracture if it is the matrix permeability which is smaller, following the ideas in [6].

Concerning space discretization we use a locally conservative finite volume method for the conservation equations (18), (23), (26), (32). The advective terms are approximated using an upstream weighted cell-centered finite volume method to calculate $\mathbf{f}_i$ in equation (28) and $\mathbf{f}_\gamma$ in equation (35). For diffusion terms we use the mixed finite element method [11, 2] for approximating $\mathbf{u}_i$ in equation (19), $\mathbf{u}_\gamma$ in equation (24), $\mathbf{r}_i$ in equation (27) and $\mathbf{r}_\gamma$ in equation (34). The mixed method was implemented as a mixed-hybrid finite element method [2, 11].

Meshes were generated with the packages GHS3D/BLSURF (Laug and al, Inria-Gamma3), BLSURF producing the 2-D mesh for $\gamma$ and the boundary of $\Omega$ from which GHS3D produces the volumetric mesh.

## 5 A numerical experiment

We consider the displacement of a nonwetting fluid by a wetting fluid in a porous medium which is a cubic domain $\Omega$ with a single inclined fracture. The wetting fluid is injected through one vertical face of this cube and the fluids exit the cube through the opposite face. On the four other faces a no flow condition is imposed.

The interface plane $\gamma$ containing the fracture is perpendicular to the injection and production faces of $\Omega$, but the actual fracture itself does not go all the way up to either of these faces. It stops 1/10 of a side length from each of these faces so the length of the physical fracture is 4/5 of the horizontal length of $\gamma$.. It does however go all the way to two of the impermeable faces. The actual fracture itself is thus a rectangle lying in $\gamma$. In the part of $\gamma$ which is not the actual fracture the rock type is that of the rock matrix. Consequently we encounter two changes of rock type along $\gamma$ when moving horizontally.

The width $d$ of the fracture is two thousand times smaller than the length of the edges of $\Omega$ and its porosity $\Phi_f = 0.7$ is seven times larger than that of the rock matrix $\Phi_i = 0.1$. We used a scalar $K$ for absolute permeability that is one thousand time larger in the fracture than in the matrix rock. The Muelam-Van Genuchten model is used for the capillary pressure and relative permeability curves. Relative permeabilities as functions of the wetting phase saturation are, for both the rock matrix and the fracture,

$$k_w(s_w) = \sqrt{s_w}[1-(1-s_w^n)^m]^2, \quad k_{nw}(s_w) = (1-s_w)^2(1-s_w^n)^{2m},$$

with $n = 2.8, m = 1 - 1/n$. The capillary pressure function is of the form $\pi(s) = \sqrt{\Phi/\mathbf{K}}\left((1-s)^{-1/m}-1\right)^{1/n}$ and Fig. 1 shows the capillary pressure

curves that are used.

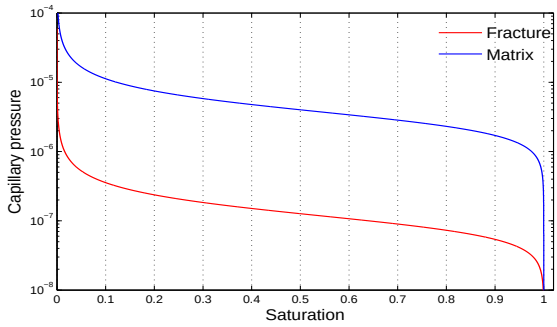


Figure 1: Capillary pressure curves

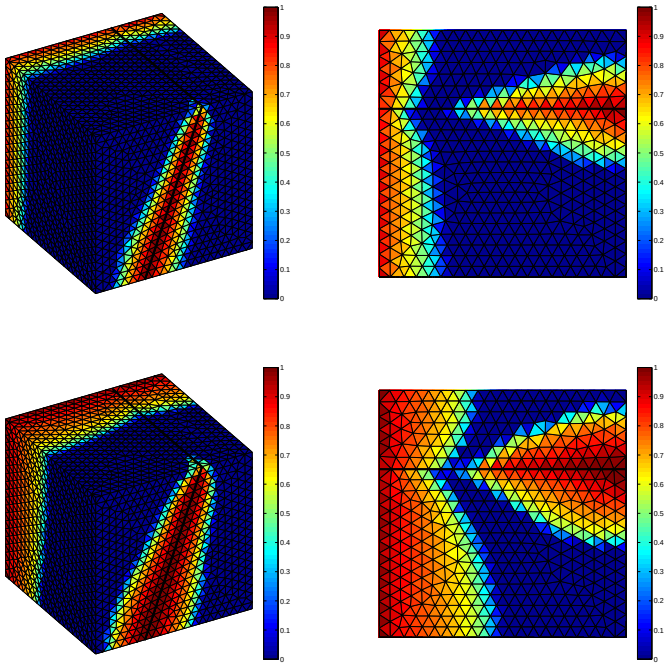

Figure 2: Saturation at two different times of the injected wetting fluid. At left saturation on $\partial\Omega$. At right saturation on the bottom face of $\Omega$.

The 2-D mesh for $\gamma$ together with the boundary of $\Omega$ has 880 triangles and from this 2-D mesh was produced a volumetric mesh with 72000 tetrahedra. Fig. 2 shows the saturation of the wetting phase at two different times. At left the saturation $s_w$ is shown on three faces of the boundary of $\Omega$ and at right we show $s_w$ on the bottom face of $\Omega$.

From equations (19), (24), (28) and (35) we note that gravity effects are proportional to the absolute permeability and therefore are more important in the fracture than in the rock matrix. This explains why we see in Fig. 2 an accumulation of the wetting fluid at the bottom of $\Omega$ near the fracture.

We observe also a cusp in the saturation isolines near the entrance of the fracture as the wetting phase is drawn into the more permeable fracture. Around the fracture exit however, the wetting phase fluid accumulates as it enters the less permeable rock matrix.

## 6 Conclusion

In this paper we presented a reduced fracture model for two-phase flow which takes into account matrix-fracture interaction, the change of rock types between the fracture and the matrix rock, and gravity effects. An example showed some of the capability of the numerical model. We refer to [1] for more details and more numerical experiments.

## REFERENCES

[1] E. Ahmed, J. Jaffré, and J. E. Roberts, *A 3-D reduced fracture model for two-phase flow in porous media*. preprint HAL 2012.

[2] F. Brezzi and M. Fortin, *Mixed and hybrid finite element methods*, Springer, 1991.

[3] G. Chavent and J. Jaffré, *Mathematical models and finite elements for reservoir simulation*, North Holland, 1986.

[4] A. Fumagalli and A. Scotti, *A numerical method for two-phase flow in fractured porous media with non-matching grids*, Advances in Water Resources, 62 (2013), pp. 454–464.

[5] R. Helmig, *Multiphase Flow and Transport Processes in the Subsurface*, Springer, 1997.

[6] T.-T.-P. Hoang, C. Japhet, M. Kern, and J. E. Roberts, *Space-time domain decomposition methods for flow and transport in porous media with*

*fractures*, in Proceedings of the 6th International Conference on Approximation Methods and Numerical Modeling in Environment and Natural Resources (Mamern VI), 2015.

[7] J. Jaffré, M. Mnejja, and J. E. Roberts, *A discrete fracture model for two-phase flow with matrix-fracture interaction*, Procedia Computer Science, 4 (2011), pp. 967–973.

[8] V. Martin, J. Jaffré, and J. E. Roberts, *Modeling fractures and barriers as interfaces for flow in porous media*, SIAM J. Sci. Comput., 26 (2005), pp. 1667–1691.

[9] J. Mondteagudu and A. Firoozabadi, *Control-volume model for simulation of water injection in fractured media: incorporating matrix heterogeneity and reservoir wettability effects*, SPE J., 12 (2007), pp. 355–366.

[10] V. Reichenberger, H. Jakobs, P. Bastian, and R. Helmig, *A mixed-dimensional finite volume method for two-phase flow in fractured porous media*, Advances in Water Resources, 29 (2006), pp. 1020–1036.

[11] J. E. Roberts and J.-M. Thomas, *Mixed and hybrid methods*, Handbook of numerical analysis, 2 (1991), pp. 523–639.

[12] X. Tunc, I. Faille, T. Gallouet, M. C. Cacas, and P. Havé, *A model for conductive faults with non-matching grids*, Computational Geosciences, 16 (2012), pp. 277–296.